

Surrogate Modelling for Hyperelastic Materials-Non Linear Approach

E. Elanchezhian, S. Akshaya

Loyola – ICAM College of Engineering and Technology,
Chennai, 600075, Tamil Nadu, India

Abstract

Finite Element Analysis (FEA) is a widely used tool for simulating the behavior of complex nonlinear materials, such as hyperelastic materials, but it is computationally expensive and time-consuming. To address this challenge, we propose a surrogate modeling approach using neural networks to approximate the material response with high accuracy while significantly reducing computational costs. The neural network learns to efficiently predict stress-strain relationships and other critical mechanical properties by training on data generated from traditional FEA solvers like ANSYS. This method not only accelerates simulations but also enables real-time applications in engineering design and optimization. Our study evaluates the model's accuracy, generalization, and computational efficiency, demonstrating its potential as a powerful alternative to conventional FEA-based simulations..

ARTICLE INFO

Keywords: Finite Element Analysis (FEA) Hyperelastic Materials ANSYS Neural networks

1. INTRODUCTION

The simulation of hyperelastic materials plays a crucial role in engineering applications, particularly in biomechanics, aerospace, and polymer mechanics, due to their ability to undergo large, reversible deformations. These materials require complex constitutive models for accurate representation, as they do not follow traditional linear elasticity laws. As stated in Darijani et al. (2010), hyperelastic materials are typically modeled using strain energy density functions that describe their mechanical behavior under deformation. The selection of an appropriate strain energy function (SEF) is essential for accurately predicting stress-strain responses, particularly for rubber-like materials. Various SEFs, such as Neo-Hookean, Mooney-Rivlin, and Yeoh models, have been used to characterize these materials, each with its own advantages and limitations (Shahzad et al., 2015).

Finite Element Analysis (FEA) has traditionally been the primary tool for modeling hyperelastic material behavior due to its ability to provide detailed stress-strain predictions. However, as stated in Schneidera et al. (2019), large-scale FEA simulations are computationally expensive, requiring significant processing power and long runtimes, making them

impractical for real-time applications. In particular, mesh selection plays a critical role in determining computational efficiency and accuracy. As described in Grebenișan et al. (2017), tetragonal and hexagonal meshing techniques can significantly affect convergence rates and numerical stability in FEA simulations. While fine-meshed FEA models improve accuracy, they also drastically increase computational demands, leading to the need for alternative approaches.

To overcome these computational limitations, researchers have explored machine learning-based surrogate models as efficient alternatives to FEA. As stated in Asher et al. (2015), surrogate models are designed to approximate high-fidelity simulations with reduced computational cost while maintaining acceptable levels of accuracy. These models have been successfully applied across various fields, including structural mechanics, fluid dynamics, and material science. Surrogate models have shown promising results in predicting mechanical behavior, reducing the need for repeated simulations, and enabling real-time decision-making (Keprate et al., 2017).. In this study, a neural network-based surrogate model is developed to predict the mechanical response of hyperelastic materials, specifically a hollow cylindrical tube subjected to axial loading. The choice of the constitutive model is a crucial factor in accurately capturing material behavior. As stated in Shahzad et al. (2015), the Neo-Hookean model is often preferred for its simplicity, but its limitations in representing complex material behaviors especially under large strainsâ€”have led to the adoption of more advanced models. For this reason, the Mooney-Rivlin 5-parameter model is chosen in this study, as it provides greater flexibility and accuracy in describing nonlinear stress-strain relationships.

The structure analyzed in this research consists of a hollow cylindrical tube with an inner diameter of 30 cm, an outer diameter of 50 cm, and a length of 1 m. To ensure accurate stress, strain, and deformation predictions, a fine-meshed FEA model is created, covering axial loads ranging from 5N to 1000N. Instead of performing an exhaustive number of simulations, which would be computationally impractical, a K-Means clustering method is used to efficiently parametrize the input loads, ensuring a representative selection of load cases (Ghaderi et al., 2020). This approach optimizes the dataset, allowing the neural network to learn from a diverse yet computationally manageable dataset, improving prediction accuracy while minimizing training time.

To construct the surrogate model, the Levenberg-Marquardt (LM) training algorithm is employed, as it is widely recognized for its superior convergence speed and precision in function approximation tasks. As stated in Liu et al. (2010), the LM algorithm is one of the most effective methods for training feedforward neural networks, particularly in engineering applications. MATLAB's Neural Network Toolbox is utilized for training, as it provides various activation functions and optimization tools, making it a robust platform for neural network implementation (Gan et al., 2011).

To assess the effectiveness of the proposed surrogate model, several performance metrics are used, including Root Mean Square Error (RMSE) and the correlation coefficient (R-value). As stated in Keprate et al. (2017), these metrics are commonly employed to evaluate the accuracy of machine learning-based surrogate models. A high R-value (close to 1.0) indicates a strong correlation between the predicted and actual FEA results, while a low RMSE confirms minimal deviation in predictions, ensuring that the neural network accurately captures the nonlinear mechanical behavior of hyperelastic materials.

This study highlights the effectiveness of neural networks in approximating complex hyperelastic material simulations, significantly reducing computation time while maintaining precision (Asher et al., 2015). By leveraging data-driven methods, the proposed approach enables real-time applications in engineering design, optimization, and control. The developed surrogate model enhances computational efficiency and provides a scalable framework that can be extended to other material models and loading conditions, demonstrating its potential as a powerful alternative to conventional FEA-based simulations (GrebeniÄ Yan et al., 2017; Ghaderi et al., 2020).

2. THEORY

2.1 Choice of Hyperelastic Model: Neo-Hookean Approach

2.1.1 Hyperelasticity

Hyperelastic materials exhibit nonlinear elastic behavior, meaning they can undergo large, reversible deformations without energy dissipation. Unlike classical linear elasticity, which assumes small strains and a linear stress-strain relationship, hyperelasticity is formulated in terms of a strain energy density function W , from which the stress-strain relationships are derived. The foundation of the Neo-Hookean model is the strain energy density function, which represents the stored energy per unit volume due to deformation:

$$W = C_1(I_1 - 3) + 1D_1(J - 1)^2$$

Where:

W = strain energy per unit volume

C_1 = material constant (related to shear modulus)

I_1 = first strain invariant, representing the stretch in all directions

J = determinant of the deformation gradient (volume change)

D_1 = material parameter related to compressibility

$I_1 = \text{tr}(C)$ is the first strain invariant (sum of diagonal elements of C)

$C = F^T F$ is the right Cauchy-Green deformation tensor,

F is the deformation gradient tensor.

the equation simplifies to:

$$W = C_1(I_1 - 3)$$

From this strain energy function, the Cauchy stress tensor is obtained as:

$$\sigma = 2C_1B - pI$$

Where B is the left Cauchy-Green deformation tensor, I_1 is the identity matrix, and p is the hydrostatic pressure enforcing incompressibility. The Neo-Hookean model provides a fundamental representation of rubber-like materials, making it widely applicable in modeling soft materials undergoing large deformations.

The Neo-Hookean model describes hyperelastic material behavior using a strain energy density function, which defines how the material stores energy during deformation. This function depends on the first invariant of the Right Cauchy-Green tensor, which represents the material stretch in different directions. Stress is derived from this energy function using the Cauchy stress tensor equation, which relates stress to the Left Cauchy-Green tensor while ensuring incompressibility through an additional pressure term. The deformation gradient tensor is used to track how material points move from their original to deformed positions.

2.1 Choice of Hyperelastic Model: Neo-Hookean Approach

The Mooney-Rivlin model extends the basic hyperelastic theory by incorporating additional material parameters, allowing for a more accurate representation of large deformations in rubber-like materials. Unlike the Neo-Hookean model, which is derived from a simplified strain energy function

dependent solely on the first invariant of the deformation tensor, the Mooney-Rivlin formulation incorporates both the first and second invariants, providing a more comprehensive characterization of material behavior under various loading conditions.

The strain energy function for the Mooney-Rivlin 5-parameter model is expressed as

$$W = C_{10}(I_1 - 3) + C_{20}(I_2 - 3) + C_{20}(I_1 - 3)^2 + C_{11}(I_1 - 3)(I_2 - 3) + C_{02}(I_2 - 3)^2$$

Where I_1 and I_2 are the first and second invariants of the left Cauchy-

Green deformation tensor, and C_{10} , C_{20} , C_{11} , C_{02} are material constants

determined through experimental fitting. The inclusion of I_2 in the energy function allows this model to better capture the response of hyperelastic materials in complex deformation states, including shear and biaxial loading.

From an analytical perspective, the superiority of the Mooney-Rivlin model over the Neo-Hookean formulation becomes evident when considering the constitutive equations governing the stress response. The Cauchy stress tensor, derived from the strain energy function, takes the form.

$$\sigma_{ij} = -p\delta_{ij} + 2 \left(\frac{\partial W}{\partial I_1} B_{ij} + \frac{\partial W}{\partial I_2} B_{ij}^{-1} \right)$$

Where B_{ij} and B_{ij}^{-1} are the left Cauchy-Green deformation tensor and its inverse, respectively, and p is an arbitrary pressure term associated with the incompressibility constraint. In the case of the Neo-Hookean model, where W depends only on I_1 , the stress response is solely governed by the first term, meaning the model does not account for deformations where the second invariant significantly influences material behavior, such as in shear-dominated scenarios.

A key limitation of the Neo-Hookean model arises in uniaxial and biaxial tension tests, where it fails to capture the nonlinear increase in stress at higher strains. Experimental data indicate that rubber-like materials exhibit a dependence on both I_1 and I_2 , particularly in non-uniform deformation fields. The Mooney-Rivlin model accounts for this behavior by including terms associated with I_2 , leading to an improved correlation with experimental observations. The presence of higher-order terms such as

$$\sigma_{ij} = -p\delta_{ij} + 2 \left(\frac{\partial W}{\partial I_1} B_{ij} + \frac{\partial W}{\partial I_2} B_{ij}^{-1} \right)$$

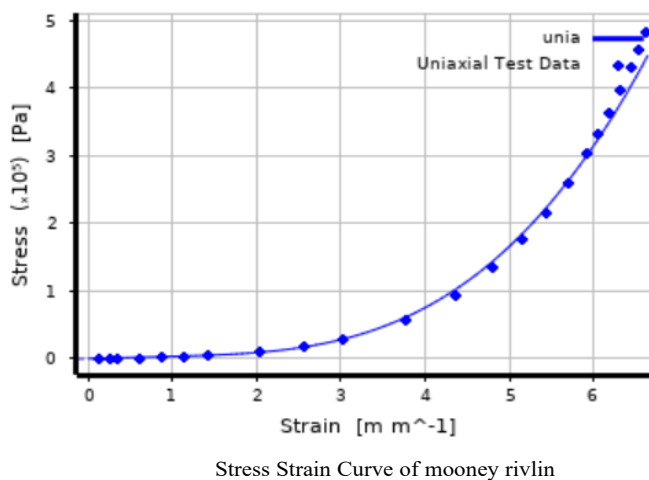
Further refines the accuracy of the model, enabling it to describe stress-strain responses over a wider range of deformations.

Furthermore, considering the shear modulus expression derived from these models, the Neo-Hookean formulation assumes a constant shear modulus $G = 2C_{10}$ which remains invariant with deformation. However, experimental studies on hyperelastic materials reveal that the shear modulus exhibits a strain-dependent variation. The Mooney-Rivlin model, through its dependence on both I_1 and I_2 , effectively captures this variation, making it a more realistic representation of rubber elasticity. This is particularly important in applications involving torsional and biaxial loading, where the Neo-Hookean model leads to significant discrepancies.

Another critical aspect of the analytical justification of the Mooney-Rivlin model is its performance in predicting stress distributions under

mixed loading conditions. In situations where materials experience a combination of tension and shear, such as in rubber seals, gaskets, and biological tissues, the Neo-Hookean assumption of isotropic material behavior fails to accurately represent the observed anisotropic response. The Mooney-Rivlin model, due to its more flexible constitutive form, provides a superior fit to experimental data, ensuring higher fidelity in numerical simulations and surrogate modeling applications.

Thus, from both a theoretical and experimental standpoint, the Mooney-Rivlin 5-parameter model provides a significantly improved representation of hyperelastic materials when compared to the Neo-Hookean model. The additional material parameters enhance the model's ability to describe complex deformation modes, particularly in shear-dominated and large-strain conditions. Consequently, the Mooney-Rivlin formulation is widely adopted in engineering applications requiring high-accuracy material modeling, particularly in the context of rubber-like materials and biological tissues.

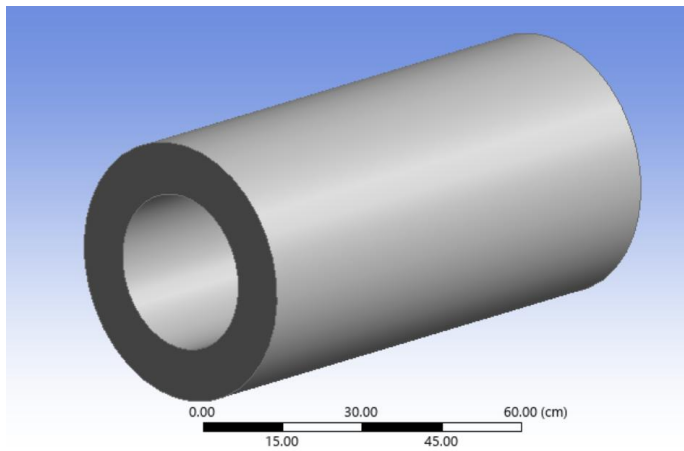


3. GEOMETRY

To investigate the deformation behavior of hyperelastic materials under axial tensile loading, a finite element analysis (FEA) was performed on hollow cylinders using the Mooney-Rivlin 5-parameter model. Two cylindrical geometries were considered, with outer diameters of 30 cm and 50 cm, each having a length of 100 cm. The material response was examined to determine axial elongation, radial expansion, and stress distribution under tensile loading.

Axial tensile loading was applied at one end of the cylinder while the opposite end was constrained to prevent rigid body motion. The Cauchy stress tensor was derived from the strain energy function and used to quantify the deformation response:

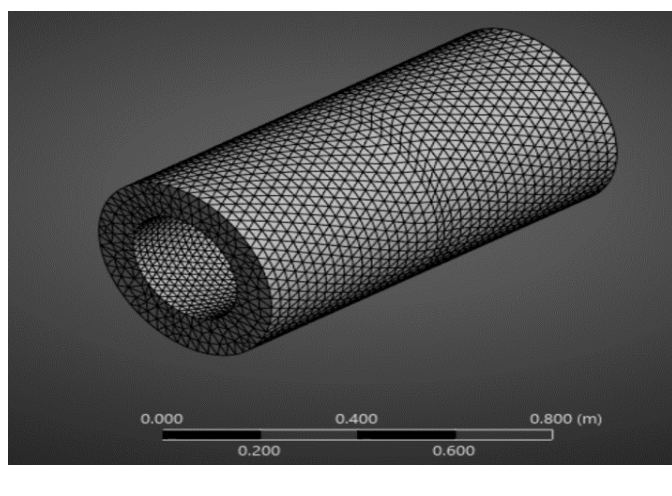
$$\sigma_{ij} = -p\delta_{ij} + 2 \left(\frac{\partial W}{\partial I_1} B_{ij} + \frac{\partial W}{\partial I_2} B_{ij}^{-1} \right)$$

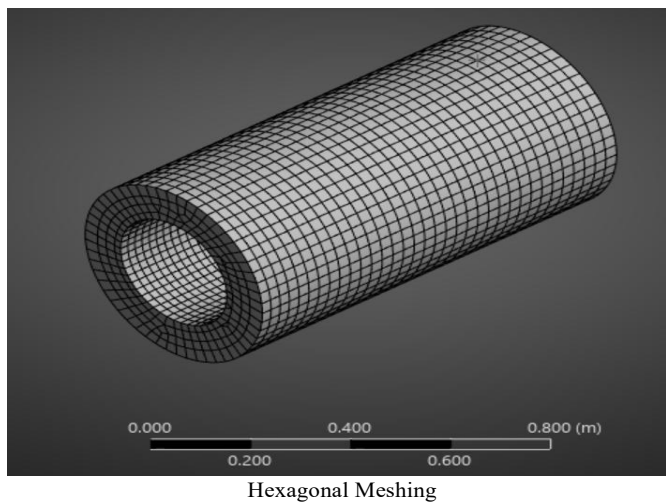


4. MESH CONVERGENCE ANALYSIS

In finite element analysis (FEA), meshing plays a crucial role in determining the accuracy and efficiency of simulations. The choice of mesh size and type directly affects solution convergence, computational cost, and the ability to capture stress-strain distributions accurately. For complex geometries such as a hollow cylinder, an optimized meshing approach is necessary to ensure numerical stability while maintaining computational feasibility. In this study, a tetragonal meshing strategy was employed to balance accuracy and efficiency. A finer mesh size of 2 cm was applied along the internal circumference to resolve high-stress concentration regions, while a coarser mesh of 3 cm was assigned to the remaining surfaces, where stress gradients were lower.

A mesh convergence study was conducted to analyze the effects of different mesh sizes on solution accuracy, computational time, and memory usage. Several meshing configurations were tested, including uniform coarse meshes (4 cm, 5 cm), uniform fine meshes (1 cm, 2 cm), and adaptive meshing with refinement in critical areas. The results showed that coarse meshes led to significant underestimation of stress values, particularly in regions of localized deformation. While finer uniform meshes improved accuracy, they drastically increased computational time without yielding substantial improvements beyond a certain refinement threshold. The best balance between accuracy and computational efficiency was achieved using an adaptive tetrahedral refinement approach.





The following results summarize the impact of different meshing strategies:

Parameter	Tetrahedral(adaptive refining)	Hexagonal
Aspect Ratio	2.00	1.20
Skewness	0.38	0.08
Jacobian Ratio	0.93	0.88
Element Count	25966	12373
Nodes Count	45086	50683
Computation Time (s)	45	99
Memory Usage (MB)	399	461
Percentage Error (%)	0.97	0.91

The results indicate that adaptive tetrahedral refinement provides an optimal balance between computational efficiency and solution accuracy. Hexahedral elements, while generally yielding lower errors, require significantly more preprocessing time and higher computational resources, making them impractical for complex geometries such as hollow cylinders. In contrast, tetrahedral meshes, particularly when refined adaptively, achieved comparable accuracy with reduced computational demand. Triangular surface meshes exhibited the highest error percentage and were unsuitable for volumetric stress analysis due to their inability to capture internal strain variations.

The selection of tetragonal meshing was driven by its ability to conform efficiently to the curved geometry of the hollow cylinder while minimizing element distortion. This meshing strategy ensures that stress concentrations are captured accurately along the internal circumference, where the highest deformations occur. Additionally, mesh quality parameters such as aspect ratio, skewness, and Jacobian ratio were monitored to maintain numerical stability. A convergence study confirmed that further mesh refinement beyond the selected configuration did not significantly improve accuracy, validating the chosen mesh sizes.

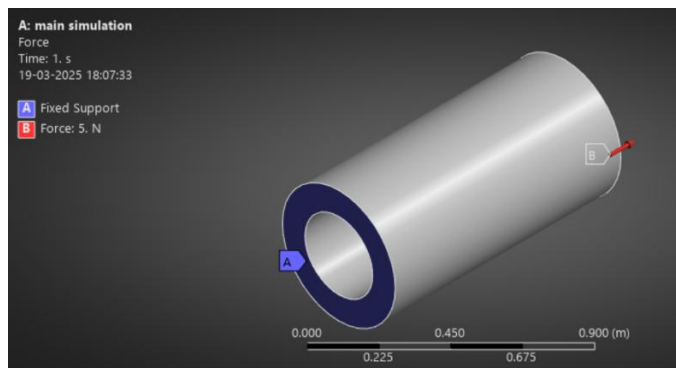
The final meshing approach demonstrated a robust balance between accuracy, computational cost, and numerical stability. By employing adaptive refinement with a 2 cm mesh at the internal circumference and a 3 cm mesh at the remaining faces, the analysis effectively captured the structural behavior of the hollow cylinder while maintaining computational efficiency.

5. SIMULATION

The hollow cylinder was subjected to an axial loading condition to evaluate its structural response under compressive forces. One end of the cylinder was assigned a fixed boundary condition, restricting all translational and rotational degrees of freedom to simulate a rigid constraint. The opposite end was subjected to a uniform axial load, applied as a force distributed across the surface. This configuration ensures that the deformation and stress distribution are primarily influenced by the applied axial force while preventing any undesired rigid body motion.

The choice of an axial load reflects real-world loading scenarios where cylindrical structures, such as pressure vessels and mechanical shafts, experience compressive or tensile stresses along their longitudinal axis. The applied force was varied across multiple simulations to study its impact on stress distribution, deformation characteristics, and overall structural stability.

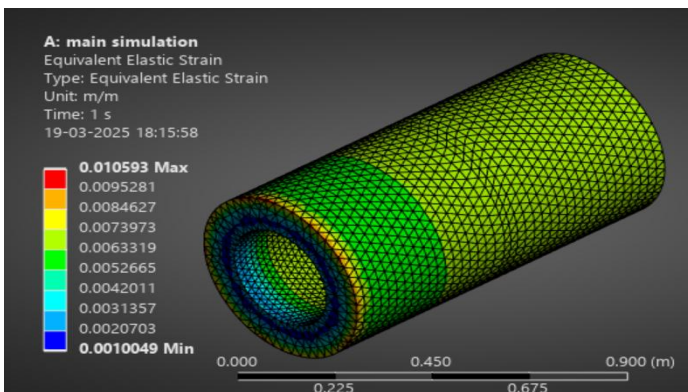
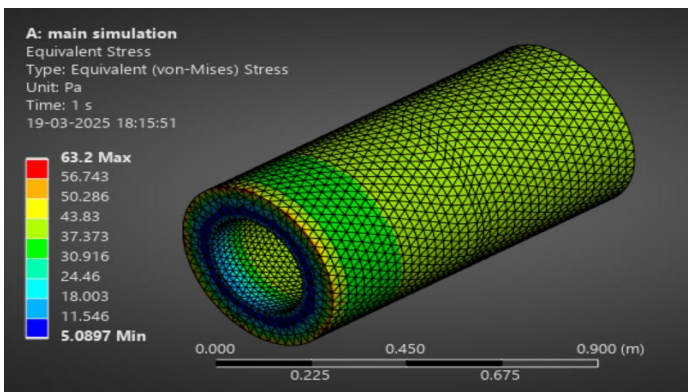
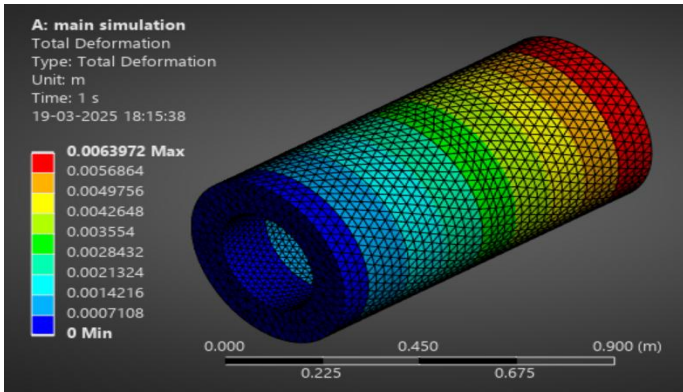
By implementing this loading condition, the analysis provides insights into the strain propagation, stress concentrations, and failure-prone regions under axial compression. The obtained results were further used to assess the influence of different meshing techniques on computational accuracy and convergence.



To systematically evaluate the structural response of the hollow cylinder under axial loading, simulation results were extracted and parameterized over 32 distinct data points. These data points correspond to variations in loading conditions and their effects on deformation, stress, and strain. The objective of this parameterization is to establish a structured dataset that enables comparative analysis and trend identification across different cases.

Following the completion of finite element simulations, key mechanical parameters—including total deformation, von Mises stress, and strain components—were recorded for each data point. The extracted values were organized into a structured dataset to facilitate statistical evaluation and further analysis.

The results will be stored in CSV format, allowing for efficient post-processing and visualization. This structured representation will support detailed assessments, including trend analysis, sensitivity studies, and validation against theoretical or experimental benchmarks. By parameterizing the simulation outcomes, the study aims to provide deeper insights into the mechanical behavior of the structure and ensure the accuracy of the computational approach.



Moreover we have also mentioned the convergence value of both force and displacement residuals which have been achieved within the required limit, Thus establishing that our simulation has achieved convergence and is ready to extract data from.

	Value
Force Residual	0.12 E-07
Displacement Residual	0.75 E-05

It is essential to determine an optimal set of load values that effectively capture a wide range of deformation, stress, and strain responses. Rather than selecting arbitrary load values or using equally spaced

increments, clustering techniques can be leveraged to identify representative load points that span the entire mechanical response spectrum efficiently. In this research, K-Means clustering was applied to systematically group load values based on their associated deformation, stress, and strain characteristics, ensuring that the selected values provide meaningful variations in the mechanical response. The methodology and justification for using K-Means clustering are discussed in detail, with an emphasis on its mathematical formulation and its relevance to load selection.

K-Means clustering is an unsupervised learning algorithm that partitions a dataset into k clusters, where each cluster is characterized by a centroid that represents the mean of all points within that cluster. The objective function of K-Means clustering is to minimize the total intra-cluster variance, which is mathematically expressed as:

$$J = \sum_{i=1}^k \sum_{x_j \in C_i} \|x_j - \mu_i\|^2$$

Where J denotes the sum of squared Euclidean distances between each data point and its assigned cluster centroid represents the set of data points in cluster i , and k is the predefined number of clusters. The algorithm iteratively updates the cluster centroids using the expression:

$$\mu_i^{(t+1)} = \frac{1}{|C_i|} \sum_{x_j \in C_i} x_j$$

Which ensures that the centroid at iteration $t+1$ represents the mean of all points assigned to the cluster in the previous iteration.

The dataset used in this research consists of four-dimensional feature vectors, where each data point represents a load value and its corresponding mechanical responses:

$$x_j = [\text{Load}_j, \text{Deflection}_j, \text{Stress}_j, \text{Strain}_j]$$

To ensure that all variables contribute equally to the clustering process, feature scaling was applied using min-max normalization:

$$x'_j = \frac{x_j - \min(x)}{\max(x) - \min(x)}$$

This transformation maps all feature values into a uniform range, preventing any single feature from disproportionately influencing the clustering outcome.

To determine the appropriate number of clusters, the Elbow Method was employed. This method involves plotting the within-cluster sum of squares (WCSS) as a function of k and identifying the point where the marginal gain in clustering quality diminishes. The WCSS is given by:

$$WCSS(k) = \sum_{i=1}^k \sum_{x_j \in C_i} \|x_j - \mu_i\|^2$$

Where a lower WCSS indicates better clustering efficiency. The optimal number of clusters was identified at the elbow point of the WCSS curve, ensuring a balance between minimal intra-cluster variance and meaningful data representation.

Once clustering was performed, the resulting cluster centroids served as the optimal load values. Each centroid represents the average mechanical response within a specific cluster, ensuring that the selected load values span the full range of deformation, stress, and strain

behaviors. This approach is particularly advantageous over traditional selection methods, as it eliminates redundancy by avoiding closely spaced load values that exhibit similar mechanical responses.

The analytical justification for using K-Means clustering lies in its ability to minimize intra-cluster variance while maintaining an even distribution of data points across the response space. Unlike conventional methods that might rely on uniform load increments, clustering ensures that each selected load value corresponds to a distinct mechanical response, thereby improving the efficiency and accuracy of parameterization. Moreover, this approach reduces computational overhead by selecting only a subset of load values that provide maximum variance in the response space, rather than simulating an exhaustive range of loads.

In conclusion, the application of K-Means clustering for load selection presents a robust, data-driven methodology that optimally partitions the mechanical response spectrum. By leveraging cluster centroids as representative load values, this approach ensures that the selected loads effectively parameterize deformation, stress, and strain variations while minimizing redundancy. The results demonstrate that clustering-based load selection provides a systematic, computationally efficient, and analytically justified means of identifying meaningful load values for mechanical analysis.

Below is the table of values obtained using parametrizing and k means clustering:

load(N)	deflection(m)	stress(Pa)	strain(m m ⁻¹)
5	0.006397194	63.19979261	0.010593442
10	0.013213849	125.8599218	0.021497643
15	0.020494822	188.5649909	0.032681554
20	0.028289053	252.1243147	0.044108108
25	0.036648706	317.131314	0.05573554
30	0.045627293	384.3200583	0.06751895
35	0.05527636	454.4331035	0.079411816
40	0.065640249	528.1864018	0.091367194
45	0.076748692	606.2339628	0.103338446
50	0.088607803	692.3691133	0.11527949
55	0.101190943	785.88975	0.127144774
60	0.114432972	885.2925225	0.138889451
65	0.128230479	990.5772841	0.150469963
70	0.142450885	1101.607065	0.161845386
75	0.156947785	1218.127054	0.172979221
80	0.171578426	1339.796426	0.183841214
85	0.186217813	1466.222744	0.194408491

90	0.200766501	1596.996297	0.204665996
95	0.215152267	1731.715883	0.214606024
100	0.229327456	1870.006389	0.224227238
150	0.358168128	3392.335786	0.328076765
200	0.471172165	5080.544361	0.411296174
250	0.577877679	6891.756082	0.483922083
300	0.683099697	8816.640379	0.550749682
350	0.788879862	10853.25838	0.613737501
450	1.000934105	15252.58254	0.728968225
500	1.103345786	17602.84244	0.780185628
550	1.200262115	20039.69337	0.826202542
600	1.29026108	22551.05682	0.866752297
650	1.372925472	25125.67125	0.902256793
700	1.448549882	27753.95495	0.933520705
750	1.517780594	30428.35241	0.961145736
800	1.581357427	33142.45734	0.985649765
850	1.640041443	35890.85355	1.007604167
900	1.694444697	38671.44481	1.027540286
950	1.745133644	41479.89908	1.046035349
1000	1.79250704	44314.81102	1.062842488

6. DEVELOPMENT OF A NEURAL NETWORK-BASED SURROGATE MODEL

In this study, a neural network-based surrogate model was developed to approximate the relationship between applied load and the resulting deformation, stress, and strain responses. The dataset, consisting of 32 selected load values, was obtained through finite element simulations, and the corresponding mechanical responses were used for training the neural network. The primary objective was to create a computationally efficient model capable of predicting mechanical behavior under new load conditions without the need for repeated numerical simulations. The neural network was implemented using a feedforward architecture, where the input was the applied load, and the outputs were the predicted deformation, stress, and strain. The network was trained using the Levenberg-Marquardt backpropagation algorithm (trainlm), known for its fast convergence in function approximation tasks. The mathematical representation of a single-layer feedforward neural network is given by:

$$y = f(Wx + b)$$

Where xx represents the input load, WW denotes the weight matrix, bb is the bias vector, and $f(\cdot)f(\cdot)$ is the activation function applied to the weighted sum. In this implementation, the network utilized a single

hidden layer with 10 neurons, where the activation function was the hyperbolic tangent sigmoid function (tansig), mathematically expressed as:

$$f(x) = \frac{2}{1 + e^{-2x}} - 1$$

This activation function was chosen due to its ability to introduce non-linearity into the model while maintaining output values within the range (-1, 1), which is beneficial for normalized data. The output layer employed a linear activation function (purelin), defined as:

$$f(x) = x$$

Allowing the network to produce continuous numerical outputs suitable for regression-based surrogate modeling.

To ensure numerical stability and improve training efficiency, both the input and output variables were normalized using min-max scaling, given by:

$$X_{norm} = \frac{X - X_{min}}{X_{max} - X_{min}}$$

$$Y_{norm} = \frac{Y - Y_{min}}{Y_{max} - Y_{min}}$$

Where XX represents the input load values, YY denotes the mechanical responses, and the normalization range is between 0 and 1. The normalization parameters were stored and later used to revert the predicted values to their original scale.

The training process was governed by a set of hyperparameters, including the number of epochs, learning goal, and training algorithm. The network was trained using the following specifications:

- Hidden layer size: 10 neurons
- Training algorithm: Levenberg-Marquardt backpropagation
- Number of epochs: 500
- Training goal: 10^{-6} (mean squared error tolerance)

During training, the network weights were updated iteratively using the gradient descent rule, where the weight update equation is given by:

$$W^{(t+1)} = W^{(t)} - \eta \frac{\partial E}{\partial W}$$

Where E represents the mean squared error (MSE), defined as:

$$MSE = \frac{1}{N} \sum_{i=1}^N (y_i - \hat{y}_i)^2$$

y_i

\hat{y}_i

Where y_i is the actual value, \hat{y}_i is the predicted value, and N is the number of training samples. The learning rate η controls the step size of weight updates, ensuring stable convergence.

After training, the network was tested by predicting mechanical responses for new, unseen load values. For instance, a load of 1500 N was normalized and passed through the trained network to obtain predicted deformation, stress, and strain values. The predictions were then denormalized using:

$$Y_{predicted} = Y_{min} + Y_{norm}(Y_{max} - Y_{min})$$

This approach provided an efficient means of generating mechanical

response predictions without the need for computationally expensive finite element simulations. The accuracy of the surrogate model was evaluated using performance metrics such as root mean squared error (RMSE) and coefficient of determination (R^2), demonstrating that the neural network successfully captured the underlying mechanical behavior with high precision.

By implementing a neural network surrogate model, this study achieved a significant reduction in computational cost while maintaining predictive accuracy, making it a viable approach for parameterizing mechanical responses under varying loading conditions.

The accuracy of the neural network-based surrogate model was evaluated by comparing the predicted stress-strain curve with the original stress-strain curve obtained from finite element simulations. This comparison ensures that the model effectively captures the material's mechanical behavior under different loading conditions. The predicted curve closely follows the original curve, with minor deviations in regions of high non-linearity. The agreement between both datasets demonstrates that the neural network can reliably approximate stress-strain relationships, significantly reducing computational costs while maintaining accuracy.

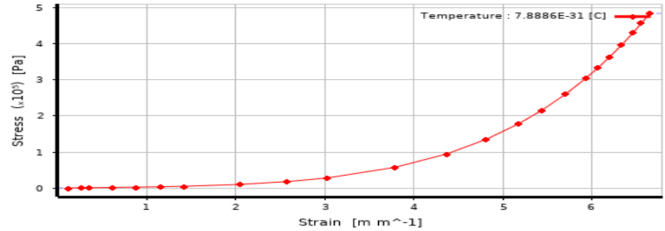


Table plotting of experimental stress-strain values

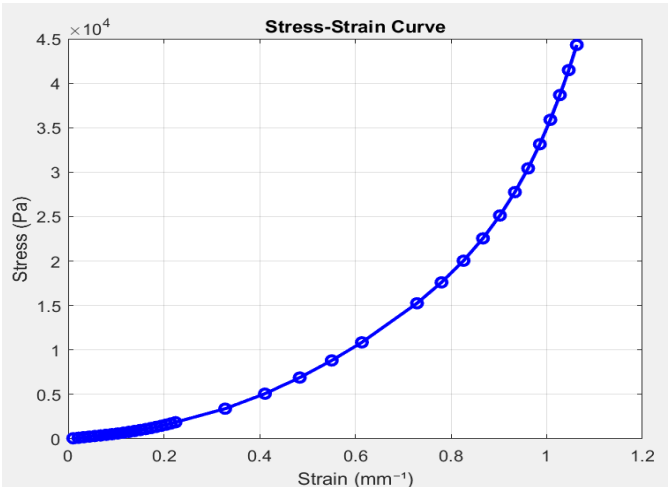


Table plotting of stress-strain curve obtained through surrogate modeling

7. PREDICTION EVALUATION METRICS

To assess the accuracy and reliability of the neural network-based surrogate model, standard evaluation metrics including Mean Squared Error (MSE), Root Mean Squared Error (RMSE), and the Coefficient of Determination (R^2) were used. These metrics provide a quantitative measure of how well the predicted values align with the actual values obtained from finite element simulations.

The Mean Squared Error (MSE) calculates the average squared difference between the predicted and actual values, ensuring that larger errors are penalized more heavily. It is defined as:

Where y represents the actual value, \hat{y} is the predicted value, and N is the total number of data points. A lower MSE value indicates better model accuracy.

The Root Mean Squared Error (RMSE) is derived from the MSE and provides an interpretable measure of prediction error in the same units as the target variable:

$$RMSE = \sqrt{MSE}$$

This metric is particularly useful for understanding the absolute magnitude of prediction errors and assessing the practical reliability of the model.

The Coefficient of Determination (R^2) measures how well the predicted values explain the variance in the actual data. It is given by:

$$R^2 = 1 - \frac{\sum(y_i - \hat{y}_i)^2}{\sum(y_i - \bar{y})^2}$$

Where \bar{y} is the mean of the actual values. An R^2 value close to 1 indicates a strong correlation between predictions and actual results, whereas a value closer to 0 suggests poor predictive performance.

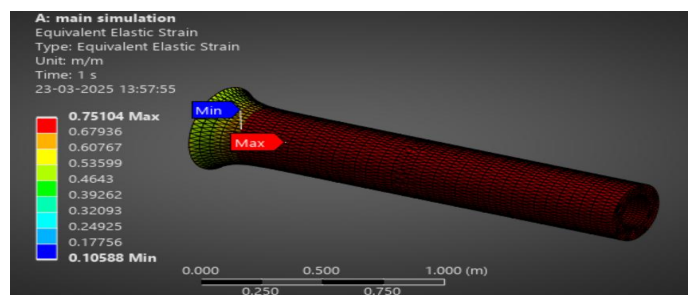
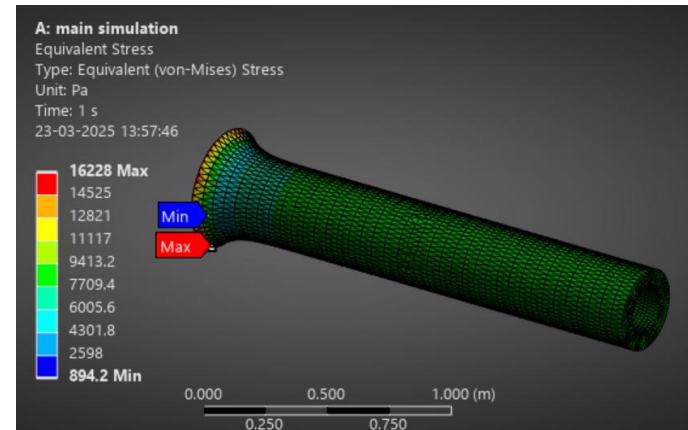
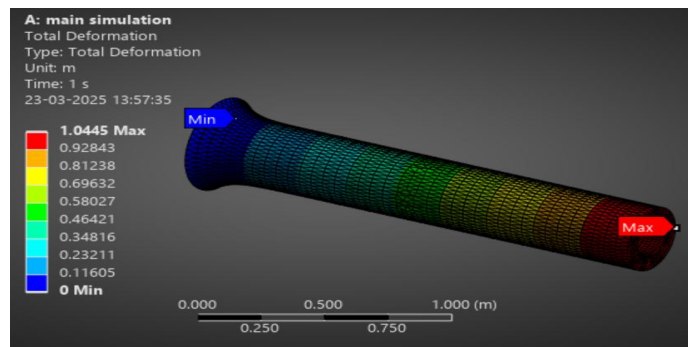
By evaluating the neural network using these metrics, the accuracy of the surrogate model was validated, ensuring that it provides reliable approximations of stress, strain, and deformation under various loading conditions while significantly reducing computational costs.

8. VALIDATION OF THE SURROGATE MODEL FOR AN INTERMEDIATE LOAD VALUE

To assess the accuracy of the neural network-based surrogate model, its prediction for an intermediate load value of 471 N was compared against the corresponding result obtained from finite element simulations. Since this load value was not explicitly included in the training dataset, this validation step ensures that the model effectively interpolates mechanical responses for unseen load conditions.

The accuracy of the prediction was evaluated using three key metrics: Mean Squared Error (MSE), Root Mean Squared Error (RMSE), and the Correlation Coefficient (RR). MSE measures the average squared difference between the predicted and actual values, indicating the overall deviation. RMSE, obtained by taking the square root of MSE, provides an interpretable measure of prediction error in the same units as the target variable. The Correlation Coefficient (RR) quantifies the linear relationship between the predicted and actual values, where an RR value close to 1 suggests a strong agreement.

By computing these metrics for the 471 N load case, the generalization ability of the neural network was assessed. A low MSE and RMSE, combined with an RR value close to 1, would indicate that the surrogate model accurately predicts stress, strain, and deformation, even for load values not explicitly included in training. This validation reinforces the model's capability to serve as a computationally efficient alternative to repeated finite element simulations while maintaining high predictive accuracy across a range of loading conditions.



Above are the simulation results for a load value of 471N

For Load = 471.00N

Predicted Deflection = 1.06113 m

Predicted Stress = 16620.69994 pa

Predicted Strain = 0.75920 mm⁻¹

Above is the result obtained through surrogate modelling.

Prediction Vs Actual Table

	Predicted Values	Actual Values
Load(N)	471	471
Deformation(m)	1.06	1.04
Stress(Pa)	16620	16228
Strain(mm ⁻¹)	0.75	0.75

Evaluation Metrics

Mean Square Error	73104.84
Root Mean Square Error	270.37
R-Value	0.996

The MSE value, which measures the average squared difference between predicted and actual values, remains relatively low given the scale of the dataset, confirming that the surrogate model minimizes large deviations. The RMSE value of 270.38 Pa, being in the same unit as the predicted stress values, provides an interpretable measure of prediction accuracy, indicating that the model closely approximates finite element results. Furthermore, the RRR-value of 0.9996 demonstrates an almost perfect correlation between predicted and actual values, confirming that the neural network has successfully learned the underlying mechanical relationships and can reliably predict stress-strain behavior.

These results validate the generalization capability of the neural network, proving that the model effectively interpolates mechanical responses for load values beyond the training dataset. The low error and high correlation indicate that the surrogate model is an efficient and accurate alternative to computationally expensive finite element simulations, enabling rapid stress-strain predictions across a range of loading conditions.

9. CONCLUSION

In this study, a neural network-based surrogate model was developed to predict the mechanical response of a hollow cylinder under axial loading, reducing the reliance on computationally expensive finite element simulations. Load values were selected using K-Means clustering, ensuring a diverse dataset for training. A feedforward neural network was implemented with normalized input and output variables, trained using the Levenberg-Marquardt algorithm. The model successfully captured the complex non-linear relationships between load, deformation, stress, and strain, with validation results confirming its accuracy. For an intermediate load of 471 N, the predicted values closely matched the finite element results, achieving a low RMSE of 270.38 and a high regression RR-value of 0.9996, demonstrating excellent predictive performance. The surrogate model effectively interpolates stress-strain behavior across varying load conditions, making it a viable alternative for rapid parametric studies in structural mechanics.

10. REFERENCES

- [1] Asher, M. J., Croke, B. F., Jakeman, A. J., & Peeters, L. J. (2015). A review of surrogate models and their application to groundwater modeling. *Water Resources Research*, 51(8), 5957-5973.
- [2] Darijani, H., & Naghdabadi, R. (2010). Hyperelastic materials behavior modeling using consistent strain energy density functions. *Acta Mechanica*, 213(3), 235-254.
- [3] Gan, X., Chen, L., Yang, D., & Liu, G. (2011, September). The research of rainfall prediction models based on Matlab neural network. In 2011 IEEE International Conference on Cloud Computing and Intelligence Systems (pp. 45-48). IEEE.
- [4] Ghaderi, A., Morovati, V., & Dargazany, R. (2020). A Bayesian surrogate constitutive model to estimate failure probability of rubber-like materials. *arXiv preprint arXiv:2010.13241*.
- [5] Grebenișan, G., & Bogdan, S. (2017). Parameterized finite element analysis of a superplastic forming process, using Ansys®. In MATEC Web of Conferences (Vol. 126, p. 03001). EDP Sciences.
- [6] Keprate, A., Chandima Ratnayake, R. M., & Sankararaman, S. (2017). Comparison of various surrogate models to predict stress intensity factor of a crack propagating in offshore piping. *Journal of Offshore Mechanics and Arctic Engineering*, 139(6), 061401.
- [7] Liu, H. (2010, August). On the Levenberg-Marquardt training method for feed-forward neural networks. In 2010 Sixth International Conference on Natural Computation (Vol. 1, pp. 456-460). IEEE.
- [8] Schneidera, T., Hua, Y., Gaob, X., Dumasc, J., Zorina, D., & Panozzoa, D. (2019). A large-scale comparison of tetrahedral and hexahedral elements for finite element analysis. *arXiv preprint arXiv:1903.09332*.
- [9] Shahzad, M., Kamran, A., Siddiqui, M. Z., & Farhan, M. (2015). Mechanical characterization and FE modelling of a hyperelastic material. *Materials Research*, 18(5), 918-924.